

New Approach to Rock Classification Based on Sparse Representations

Wognin Joseph Vangah¹ , Bi G. Théodore Toa², Alico Nango Jérôme³, Ouattara Sie⁴, Alain Clément⁵

¹Unité de Recherche et d'expertise Numérique (UREN), Université Virtuelle de Côte d'Ivoire (UVCI), Abidjan, Côte d'Ivoire

²UFR Sciences et technologique, Département de Physique, Université polytechnique de Man (UPM), Man, Côte d'Ivoire

³Classe Préparatoire des Grandes Ecoles (CPGE), Université de San Pédro (USP), San Pédro, Côte d'Ivoire

⁴Institut National Polytechnique Houphouët (INPHB), Yamoussoukro, Côte d'Ivoire

⁵Laboratoire Angevin de Recherche en Ingénierie des Systèmes (LARIS), Institut Universitaire de Technologie (IUT), Université d'Angers, Angers, France

Email: joseph.vangah@uvci.edu.ci

How to cite this paper: Vangah, W.J., Toa, B.G.T., Jérôme, A.N., Sie, O. and Clément, A. (2024) New Approach to Rock Classification Based on Sparse Representations. *Open Journal of Applied Sciences*, 14, 145-158. <https://doi.org/10.4236/ojapps.2024.141011>

Received: December 20, 2023

Accepted: January 28, 2024

Published: January 31, 2024

Copyright © 2024 by author(s) and Scientific Research Publishing Inc. This work is licensed under the Creative Commons Attribution International License (CC BY 4.0).

<http://creativecommons.org/licenses/by/4.0/>



Open Access

Abstract

In geology, classification and lithological recognition of rocks plays an important role in the area of oil and gas exploration, mineral exploration and geological analysis. In other fields of activity such as construction and decoration, this classification makes sense and fully plays its role. However, this classification is slow, approximate and subjective. Automatic classification curbs this subjectivity and fills this gap by offering methods that reflect human perception. We propose a new approach to rock classification based on direct-view images of rocks. The aim is to take advantage of feature extraction methods to estimate a rock dictionary. In this work, we have developed a classification method obtained by concatenating four (4) K-SVD variants into a single signature. This method is based on the K-SVD algorithm combined with four (4) feature extraction techniques: DCT, Gabor filters, D-ALBPCSF and G-ALBPCSF, resulting in the four (4) variants named K-Gabor, K-DCT, KD-ALBPCSF and KD-ALBPCSF respectively. In this work, we developed a classification method obtained by concatenating four (4) variants of K-SVD. The performance of our method was evaluated on the basis of performance indicators such as accuracy with other 96% success rate.

Keywords

Rock Recognition, Dictionary, Signature, Color Texture, K-SVD Variants, KD-ALBPCSF Et KG-ALBPCSF

1. Introduction

Rock classification is a key issue for the geology industry and all fields of activity.

Traditionally, rock classification and characterization is done visually following a long process by geologists and mineralogists with many years' experience and/or through laboratory tests [1]. This classification so-called manual, slow and subjective classification is subject to errors. Automatic classification, by means of dictionary computation and machine learning, a sub-field of artificial intelligence (AI) in which computers learn without being explicitly programmed [2], appears as an alternative, a consistent response to this problem.

Several fields of activity are covered (biomedical [3], facial recognition [4] and fingerprints, etc.). Machine learning has been successfully applied to the analysis of natural phenomena such as potential earthquakes [5], volcanic eruptions [6], classification of seabed mud volcanoes [7] and mining prospects [8]. However, only a few research projects using computer vision and image processing are concerned with rock classification [1] [9] [10] [11] [12] [13]. In [14], Galdames *et al.* performed a lithological classification with SVM based on textural and colorimetric analysis coupled with 3D laser features to determine the approximate mineralogical composition of rocks. Spectral classification and supervised learning techniques such as neural network methods have been used to extract features from the spectral data of rock minerals, enabling faster and more objective identification [10]. However, these methods are often tied to manually extracted rock features, which limit their adaptability to a wide variety of characteristics. The authors of [15] proposed a lightweight convolutional neural network (ShuffleNet) in deep learning, combined with the transfer learning method from images obtained with a smartphone, to perform rock image classification. However, the study carried out by these authors, which is a smartphone application, although it solves the problem of time in the recognition process and the terrain-related hazards faced by geologists, remains limited in the face of a multi-sample dataset.

This is mainly due to the great complexity of rocks, making them difficult to classify. To the best of our knowledge, however, there are as yet no works in which dictionaries containing rock signatures are estimated by highlighting reconstruction error as a discriminating factor, and where dictionary updating is done to adapt rock characteristics. Rock classification using Machine Learning systems and algorithms yielded promising results in 2005 with L episto [16]. In his study, he used Gabor filters for texture feature analysis and extraction, followed by classifiers for rock classification. Good classification is always preceded by discriminative texture/color feature extraction methods robust to noise, rotation and illumination change. For more accurate classification, [17] has proposed texture/color feature extraction methods named D_ALBPCSF and G_ALBPCSF obtained by combining statistical and frequency descriptors on direct view images of magmatic and metamorphic rocks.

This is mainly due to the great complexity of the rocks, making them difficult to classify. But to our knowledge, there is no works yet in which dictionaries containing rock signatures are estimated by highlighting reconstruction error as a discriminating factor and where dictionary updating is done to adapt rock

characteristics. Rock classification using Machine Learning systems and algorithms yielded promising results in 2005 with L episto [16]. In his study, he used Gabor filters for texture feature analysis and extraction, followed by classifiers for rock classification. Good classification is always preceded by discriminative texture/color feature extraction methods robust to noise, rotation and illumination change. For more precise classification, [17] proposed methods for extracting color texture features named D_ALBPCSF and G_ALBPCSF obtained by combining statistical and frequency descriptors on direct view images of magmatic and metamorphic rocks. For other classification and indexing algorithms such as, boosting algorithms (LPBoosting) [18], K-nearest neighbors (K-NN) [19], K-means [20] and neural networks [10], features are derived from the measurement of attributes such as energy, entropy, contrast, etc. More repetitively, feature extraction methods are based on three forms of visual attribute analysis: spectral analysis, radiometric analysis and textural analysis in the joint or separate use of color and texture. In [21], Ishikawa and Virginia in 2013, based on these visual attributes (texture and color) and Raman spectroscopy, were able to differentiate minerals from igneous rocks through analysis of the minerals' spectral signature using neural networks. However, even if mineral classification has been largely successful, it is difficult to apply the same methods to all rocks, as spectra may present a combination of competing signatures. In [22], Blake *et al.* (2012), using X-ray diffraction, required rock samples to be collected and pulverized prior to chemical analysis. However, this method is destructive and, in my view, should not be popularized. In [23], the authors evaluated several methods obtained with a convolutional neural network and Deep Learning with an accuracy of over 95% in the classification of plutonic rocks.

The authors of [24] and [25] use convolutional neural network models to classify rocks containing a background. The limitations of these methods are linked to the influence of background disturbances, background interference and the selection of sampling points. Despite much work in these areas, the problem remains unresolved. A number of segmentation and dictionary learning strategies have been developed in the literature. Suggested methods include: Artificial Neural Networks (ANNs) [13], SVM [25] [26], decision trees [24] [26], K-nearest neighbor (K-NN) [19] [26] [27], K-means [20], boosting algorithms [18], Maximum Likelihood (ML), etc. These methods, for the most part, are combined in a single algorithm. Most of these methods are combined with dimension reduction methods such as principal component analysis (PCA) or genetic algorithms (GA). These combinations help in classification. However, in some cases, these dimension reduction methods introduce noise into the classification process. Some of the algorithms used for classification are like black boxes, where it is difficult to control intermediate processes or even guarantee a good decision with a high number of color texture descriptors and redundant sample data. In an attempt to solve these problems, we explore parsimonious representations by determining learned dictionaries.

In this paper, rock classification through the implemented methods shows the effectiveness of Machine Learning (ML) with machine learning and dictionary estimation. The proposed rock recognition method is based on dictionary estimation with K-SVD [28] [29] applied to the color LBP combination and frequency transforms [17], considering the reconstruction error (lower error), allowing correlation between learned dictionaries, as a discriminating factor.

In Session II, the materials and methods used are analyzed. Section III presents the simulation results and discussion, while Section IV concludes this study and announces future work.

2. Materials and Methods

2.1. Magmatic and Metamorphic Rocks

Our study concerns igneous rocks and metamorphic rocks. Indeed, igneous rocks result from the crystallization of magma at depth (intrusive rock) and on the surface of the earth (extrusive rock). The intrusive igneous rocks that we want to recognize by image processing have a more pronounced granularity than those of extrusive igneous rocks. However, metamorphic rocks, with even less grainy textures, are the result of the transformation of igneous or sedimentary rocks under the influence of heating, increased pressure.

2.2. Organization of Images

The experimental study was conducted with a data set comprising eight (8) classes of direct-view digital images of magmatic (granite, granodiorite, gabbro) and metamorphic (schist, cipolin, migmatite, eclogite, hornfels) rocks, totalling eighty (80) images. This grouping into eight (8) classes was made by an expert geologist, taking into account certain objective characteristics of textures and colors. Each rock image in “jpg” format is cropped to a size of 256 * 256 pixels, and a sample of each image class is shown in **Figure 1**.

Table 1 shows the number of images used per class for training and model validation.

Table 1. Number of images for training and testing.

Class	Number of images for training	Number of images for the test
Class 1: Granite	10	5
Class 2: Gabbro	10	5
Class 3: Granodiorite	10	5
Class 4: Shale	10	5
Class 5: Eclogite	10	5
Class 6: Migmatite	10	5
Class 7: Corneal	10	5
Class 8: Cipolin	10	5
Total	80	40



Figure 1. Examples of the eight (8) different classes of rock images.

The experiment was carried out using the MATLAB programming language on an HP Notebook computer and processor: Intel (R) Core (TM) i5-7200U CPU @ 2.50 GHz, 2701 MHz, 2 core(s), 4 logic processor(s).

2.3. Colors Texture Descriptors

LBP descriptors and its variants have shown that they can describe textural patterns in images quite well [26]. Studies carried out in 2019 by [17] made it possible to take into account, in addition to texture and color features, the directionality present in rock images by proposing new extraction methods such as D_ALBPCSF and G_ALBPCSF. This testifies to the robustness and capability of local binary patterns.

2.4. Dictionary and Reconstruction Error Estimation

Dictionary construction is the first step in a parsimonious representation. Dictionary learning is an essential step in obtaining a quality dictionary for a particular type of data [28] [29]. The dictionary learns the patterns present in an image and provides a basis for parsimonious decomposition. It will enable the characteristic elements of a rock image to be grouped together and used as a learning base. The main idea is for the dictionary to provide a base in which the associated rock is better represented than the others. During classification, we look for the dictionary that minimizes the reconstruction error for an imposed parsimony constraint. The smaller the error, the more suitable the dictionary. In our approach, coefficients are obtained by decomposing the signal on the basis of elementary signals called “atoms”. Four types of dictionary (Gabor, DCT, G-ALBPCSF and D-ALBPCSF) have been estimated, giving rise to four methods: K-DCT, K-Gabor, KG-ALBPCSF and KD-ALBPCSF.

The proposed approaches are summarized in the flow chart in **Figure 2**.

Algorithm 1 translates the principle of the classification method presented in the flowchart in **Figure 2**.

2.5. Parameters Influencing Dictionary Learning and Error Estimation

Dictionary learning is one of the most important steps in the efficient representation of image atoms. However, it can be optimized for greater efficiency. Certain parameters influence this optimization:

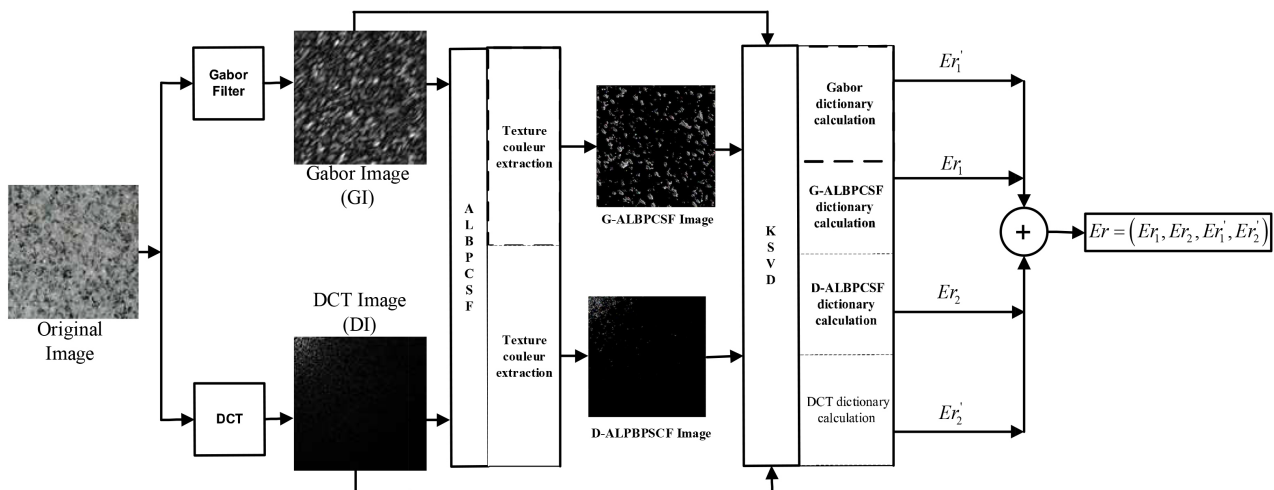


Figure 2. Flowchart of the proposed rock classification method.

Algorithm 1. KSVD_DCT_Gabor_ALBPCSF.

Input: ALBPCSF image, RGB image, DCT image, Gabor image

Output: Image dictionaries

Start

1. Apply the DCT_Gabor_ALBPCSF to ALBPCSF and RGB images.
2. Create the image database from DCT, Gabor and 1.
3. for each image in the image database.
4. Apply K-SVD to obtain the dictionary and reconstruction error
5. Save the reconstruction error in the Er vector
6. End For

End.

- The stopping criterion or number of iterations, set at 500 in this study.
- As the number of atoms K increases ($K = 75$ atoms here) while keeping the parsimony (or constraint) L at 3, the reconstruction error increases and the algorithm does not converge. As a result, there is no dictionary stability. However, when the parameter K is decreased ($K = 25$ atoms, for example), the algorithms converge and the reconstruction error is lower.
- Increasing or decreasing the size of the dictionary results in an efficient determination of the number of atoms in the dictionary. The size of the rock dictionary influences dictionary estimation, *i.e.* the larger the image size, the greater the error.

2.6. Multi-Algorithm Systems

Feature vector fusion can be performed in several ways [27] [28]. The one we are interested in here is multi-algorithm fusion. This is the most classical type of system used by many approaches. Signatures are extracted via different algorithms and then merged to give a single feature vector, providing higher accuracies than a single algorithm in rock image classification [27].

3. Experimentation and Simulation Results

Our method consists of learning the model on $2N$ observations and then validating the model on N observations. Rock classification is obtained by searching for proximity between the reconstruction errors the Euclidean distance (Equation (1)), which we found to be simple and better than the Manhattan and Minkowski distances.

$$d(A, B_k) = \left(\sum_{i=1}^N (a_i - b_{ik})^2 \right)^{\frac{1}{2}} \quad (1)$$

where a_i represents the coordinates of A (or query vector of the current rock to be identified) and b_{ik} the coordinates of B_k (reference vectors of the k rock classes in the database). To estimate the class of a rock image I to be classified, our method consists of taking into account the reconstruction errors of the rocks of the different classes. Indeed, the Euclidean distance between two (2) signature vectors A and B_k of size N , noted $d(A, B_k)$ where k describes rock classes from 1 to 8. For classification, we retain the class which has the minimum distance with image I . Let X be a vector matrix that groups on each row the reconstruction errors for each rock sample obtained over 10 trials for the 80 rock samples, *i.e.* a total of 800 values. Note that the error for each trial is obtained after 500 iterations. Let Y be a vector that groups together the average of the reconstruction errors for each sample after 10 trials on each line.

$Y = F_k$ represents the signature of each K-SVD variant. Y_{ref} contains the signature of each rock class. Note that Y_{ref} has a total of 8 values. This experiment involved 640 crosses of rock reconstruction errors.

Model performance is evaluated and compared in terms of correct classification rates: the measures of accuracy, specificity, sensitivity and error rate, based on the reconstruction errors calculated when estimating the various dictionaries of the different rocks used and learned. These performance measures defined in [17] are presented for the four methods in **Table 2**.

The results of the experimental activity presented above show that our dictionary estimation approaches for the classification of igneous and metamorphic rocks with the proposed combinations of methods, *i.e.* KD-ALBPCSF and KG-ALBPCSF, improve on the results obtained with K-DCT and K-Gabor taken individually. These results reveal once again that rock classification is a demanding and very difficult task.

Table 2. Performance indicators of the four methods for the different classes.

Methods used	Performance indicators			
	Sensitivity	Specificity	Exactness	Error rate
Gabor	0.25	0.89	0.81	0.19
DCT	0.29	0.90	0.82	0.18
KD-ALBPCSF	0.41	0.92	0.85	0.15
KG-ALBPCSF	0.50	0.93	0.88	0.12

In order to better discriminate between rocks, we concatenated the rock characteristics from the different variants used for the different experiments already carried out on 120 images from the training and test bases.

- Learning step:

In the learning step, the signatures of the different rocks class are generated: X , F and Y_{ref} .

X is the matrix of reconstruction errors for all 8 rock classes, and for the 4 variants, we have: X_1, X_2, X_3, X_4 . Each row of this matrix contains the reconstruction errors for each rock class; each of these 10 columns represents the reconstruction errors for each trial after 500 iterations.

$F = [F_1, F_2, F_3, F_4]$ represents the concatenation of the characteristic parameters of each rock from the 4 variants of K-SVD for the learning step where F_1, F_2, F_3 and F_4 each represent the average of the reconstruction errors of each variant.

Y_{ref} is the reference or signature of each rock class and X_k designates the matrix of all reconstruction errors of the 8 rock classes for each method. These different parameters are presented below.

$$Y_{ref} = \begin{bmatrix} Y_{11} & Y_{21} & Y_{31} & Y_{41} \\ Y_{12} & Y_{22} & Y_{32} & Y_{42} \\ Y_{13} & Y_{23} & Y_{33} & Y_{43} \\ Y_{14} & Y_{24} & Y_{34} & Y_{44} \\ Y_{15} & Y_{25} & Y_{35} & Y_{45} \\ Y_{16} & Y_{26} & Y_{36} & Y_{46} \\ Y_{17} & Y_{27} & Y_{37} & Y_{47} \\ Y_{18} & Y_{28} & Y_{38} & Y_{48} \end{bmatrix} \begin{matrix} \rightarrow \text{Class 1} \\ \cdot \\ \cdot \\ \cdot \\ \cdot \\ \cdot \\ \cdot \\ \rightarrow \text{Class 8} \end{matrix}$$

$$X_k = (x_{ij}^k) \text{ telle que } \begin{cases} i = 1, \dots, 10; \text{ ou } i \text{ represente la colonne} \\ j = 1, \dots, 8; \text{ ou } j \text{ represente la ligne} \\ k = 1, 2, 3, 4; \text{ ou } k \text{ represente l'indice de la methode} \end{cases}$$

For our experiment, the Y_{ref} matrix contains 8 rows, 4 columns, presented as follows:

$$Y_{ref} = \begin{pmatrix} 5.0298 & 6.6733 & 1.9231 & 5.1948 \\ 6.2540 & 7.5880 & 1.6086 & 7.5937 \\ 5.4711 & 10.8690 & 1.4577 & 8.2089 \\ 4.7049 & 4.4742 & 1.5750 & 2.4970 \\ 3.8894 & 4.7743 & 1.6374 & 1.7804 \\ 6.1953 & 7.0282 & 1.4707 & 4.3798 \\ 4.4897 & 4.3354 & 1.9379 & 1.4806 \\ 3.8759 & 4.4458 & 1.9445 & 3.0411 \end{pmatrix}$$

However, X_k matrices are matrices of 80 rows and 10 columns. An overview of these matrices, in the same dimensions as the Y_{ref} matrix, for example X_1 corresponding to one of the variants of K-SVD, is defined as follows:

$$X_1 = \begin{bmatrix} 5.0793 & 4.9441 & 4.885 & 4.9782 \\ 4.8398 & 5.0172 & 4.645 & 4.7675 \\ 5.6804 & 5.4445 & 5.4186 & 5.298 \\ 5.1769 & 5.5013 & 5.0159 & 5.1711 \\ 4.8112 & 4.9204 & 5.057 & 4.8567 \\ 5.5768 & 5.2558 & 5.2361 & 5.4207 \\ 4.6983 & 4.8746 & 4.9737 & 4.8881 \\ 5.0562 & 4.8155 & 4.8016 & 5.2816 \end{bmatrix}$$

The experiment involved comparing the reconstruction error calculated for a given rock class with all the Y_{ref} representing rock signatures, and retaining the smallest distance value from the Euclidean distance formula; this indicates the class to which the query rock belongs. **Table 3** gives the values of the performance indicators calculated to verify the performance of this combination of variants carried out on the learning phase of a set of eighty (80) rock images, each of whose eight (8) classes contains ten (10) rock images. These indicators, defined in [17], are calculated from Equations (2)-(5).

$$\text{Sensitivity} = \text{FVP} = \text{VP}/(\text{VP} + \text{FN}) \quad (2);$$

$$\text{Specificity} = \text{FVN} = \text{VN}/(\text{VN} + \text{FP}) \quad (3);$$

$$\text{Precision} = \text{VP}/(\text{VP} + \text{FP}) = \text{VN}/(\text{VN} + \text{FN}) \quad (4);$$

$$\text{Accuracy} = (\text{VP} + \text{VN})/(\text{VP} + \text{VN} + \text{FP} + \text{FN}) \quad (5);$$



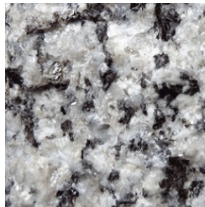

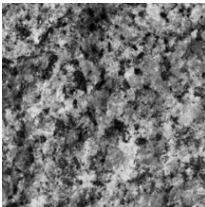

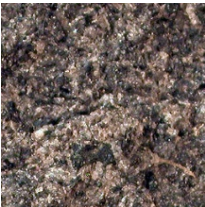



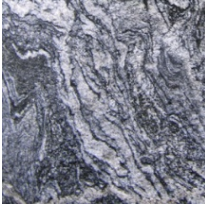







- **Test step:**

Following the same principle as the learning phase, we calculate X (X_{11} , X_{22} , X_{33} , X_{44}) for each query rock and compare these values with the Y_{ref} values. For this testing experiment, 40 rock images were used. Here, the X matrix contains 40 rows and 10 columns. An overview of one of these matrices is shown below in the form of X_{11} for the first K-SVD variant:

Table 3. Performance indicators of the combination of the 4 variants of K-SVD.

Performance indicators	Combination of the 4 variants
VP	68
VN	548
FP	12
F. N.	12
Rappel	0.85
Precision	0.85
Accuracy	0.9625
Error rate	0.0375

Table 4. Rock images used for testing.

Painting 5 - 11: Images of rocks for the test			
Granites			
	Granite_1 (A12)	Granite_2 (G)	Granite_3 (N1)
Granodiorites			
	Grano_1 (10)	Grano_2 (2)	Grano_3 (P)
Gabbros			
	Gabbro_1 (6)	Gabbro_2 (L)	Gabbro_3 (O)
Migmatites			
	Mig_1 (3)	Mig_2 (2)	Mig_3 (16)
Corneals			
	Corn_1 (9)	Corn_2 (3)	Corn_3 (11)
Eclogites			
	Hatch_1 (3)	Eclo_2 (5)	Eclo_3 (9)

Continued

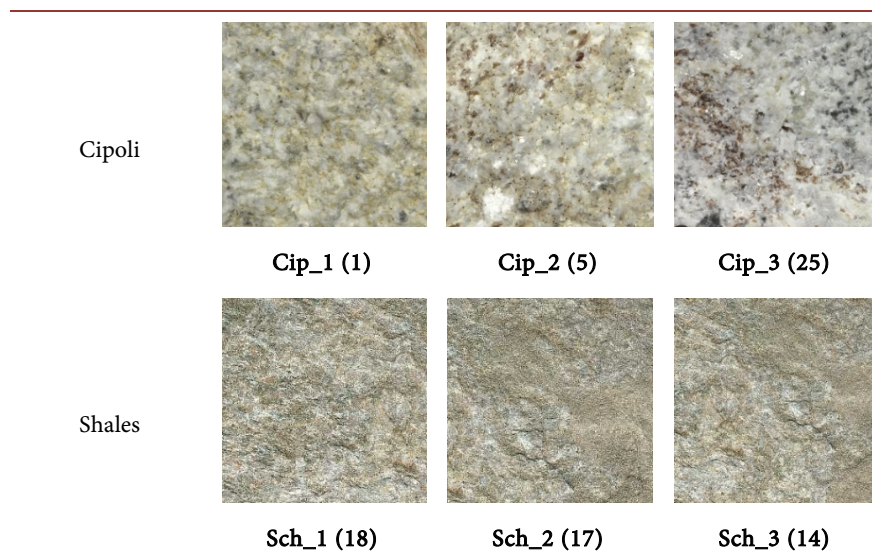


Table 5. Confusion matrix with our method.

Classes	PREDICTED CLASSES									TOTAL
	1	2	3	4	5	6	7	8		
1	5	0	0	0	0	0	0	0	0	5
2	0	4	1	0	0	0	0	0	0	5
3	0	0	5	0	0	0	0	0	0	5
4	0	0	0	2	2	0	1	0	0	5
5	0	0	0	0	4	0	0	1	0	5
6	0	2	0	0	0	3	0	0	0	5
7	0	0	0	1	0	0	4	0	0	5
8	1	0	0	0	1	1	0	2	0	5
TOTAL	6	6	6	3	7	4	5	3	0	40

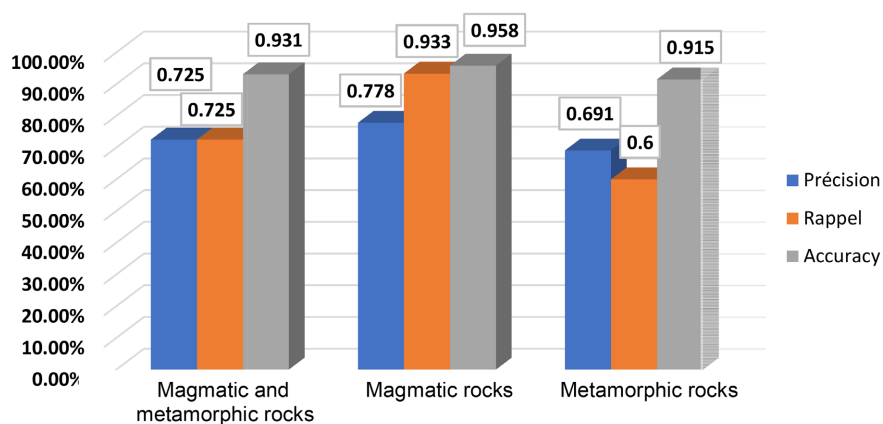


Figure 3. Average values of variant combination performance indicators.

$$X_{11} = \begin{bmatrix} 5.0793 & 4.9441 & 4.885 & 4.9782 \\ 4.8112 & 4.9204 & 5.057 & 4.8567 \\ 4.6983 & 4.8746 & 4.9737 & 4.8881 \\ 5.1459 & 4.6852 & 4.6621 & 4.9534 \\ 4.9732 & 5.0503 & 4.8245 & 4.7057 \\ 6.5739 & 6.3625 & 6.5404 & 6.5875 \\ 6.4809 & 6.4807 & 6.6571 & 6.3076 \\ 7.1768 & 7.2457 & 7.3744 & 7.2229 \end{bmatrix}$$

For the other variants, we can have, for example, as a matrix the characteristics of the various other variants X_{22} , X_{33} and X_{44} which are not presented here.

Table 4 shows some of the rock images of the different classes used for testing.

To validate our approach, a validation test is used to evaluate the combination of the four (4) K-SVD variants we propose. The results provide us with a confusion matrix for this evaluation. This confusion matrix was developed for a set of 40 rock images including 5 of each class (see **Table 5**) and **Figure 3** gives the performance indicators for verifying the suitability of the proposed method.

The results in **Table 5** show that the proposed method gives good classification performance, with an overall correct classification rate of 93.13%. However, the method classifies magmatic rocks better with a rate of 95.83%, compared to 91.5% for metamorphic rocks. The combination of methods makes up for short-fall observed with individual methods. **Figure 3** shows the average values of the various performance indicators achieved.

4. Conclusions and Future Prospects

We have proposed new classification methods that have been used in the context of the automatic classification of igneous and metamorphic rocks. The performance of these methods was evaluated through confusion matrices which resulted in classification rates. It should be noted that dictionary learning is a complex problem. Simulation shows that results are not always excellent. It is difficult to obtain the same error after two (2) trials. However, the dictionaries learned are closer to the characteristic data of the rock. Our two (2) approaches nevertheless improve the rate of correct classification by up to 50%. The concatenation of the four (4) K-SVD variants considerably improves the classification rate to 93.13% overall, with specific classification rates of 95.83% for magmatic rocks, and 91.5% for metamorphic rocks.

Looking ahead, we plan to improve the performance of our recognition method by using statistical moments as rock characteristics. We also plan to associate data obtained from signal sensors, *i.e.* the waves measured by these sensors, with rock recognition.

Conflicts of Interest

The authors declare no conflicts of interest regarding the publication of this paper.

References

- [1] Chatterjee, S., Bhattacharjee, A., Samanta, B. and Pal, S.K. (2010) Image-Based Quality Monitoring System of Limestone Ore Grades. *Computers in Industry*, **61**, 391-408. <https://doi.org/10.1016/j.compind.2009.10.003>
- [2] Geron, A. (2017) Hands-On Machine Learning with Scikit Learn and TensorFlow. O'Reilly Media, Sebastopol.
- [3] Bianconi, F. and Fernández, A. (2014) An Appendix to “Texture Databases—A Comprehensive Survey. *Pattern Recognition Letters*, **45**, 33-38. <https://doi.org/10.1016/j.patrec.2014.02.017>
- [4] Choi, J.Y., Ro, Y.M. and Plataniotis, K.N. (2012) Color Local Texture Features for Color Face Recognition. *IEEE Transactions on Image Processing*, **21**, 1366-1380. <https://doi.org/10.1109/TIP.2011.2168413>
- [5] Rouet-Leduc, B., Hulbert, C., Lubbers, N., Barros, K., Humphreys, C. and Johnson, P. (2017) Machine Learning Predicts Laboratory Earthquakes. *Geophysical Research Letters*, **44**, 9276-9282. <https://doi.org/10.1002/2017GL074677>
- [6] Ham, F., Iyengar, I., Mathewos Hambebo, B., Garces, M., Deaton, J., Perttu, A. and Williams, B. (2012) A Neurocomputing Approach for Monitoring Plinian Volcanic Eruptions Using Infrasond. *Procedia Computer Science*, **13**, 7-17. <https://doi.org/10.1016/j.procs.2012.09.109>
- [7] Lüdtke, A., Jerosch, K., Herzog, O. and Schlüter, M. (2012) Development of a Machine Learning Technique for Automatic Analysis of Seafloor Image Data: Case Example, Pogonophora Coverage at Mud Volcanoes. *Computers & Geosciences*, **39**, 120-128. <https://doi.org/10.1016/j.cageo.2011.06.020>
- [8] Zuo, R. and Carranza, E.J.M. (1967) Support Vector Machine: A Tool for Mapping Mineral Prospectivity. *Computers & Geosciences*, **37**, 1967-1975. <https://doi.org/10.1016/j.cageo.2010.09.014>
- [9] Mukherjee, D.P., Potapovich, Y., Levner, I. and Zhang, H. (2009) Ore Image Segmentation by Learning Image and Shape Features. *Pattern Recognition Letters*, **30**, 615-622. <https://doi.org/10.1016/j.patrec.2008.12.015>
- [10] Patel, A.K. and Chatterjee, S. (2016) Computer Vision-Based Limestone Rock-Type Classification Using Probabilistic Neural Network. *Geoscience Frontiers*, **7**, 53-60. <https://doi.org/10.1016/j.gsf.2014.10.005>
- [11] Chauhan, S., Rühaak, W., Anbergen, H., Kabdenov, A., Freise, M., Wille, T. and Sass, I. (2016) Phase Segmentation of X-Ray Computer Tomography Rock Images Using Machine Learning Techniques: An Accuracy and Performance Study. *Solid Earth*, **7**, 1125-1139. <https://doi.org/10.5194/se-7-1125-2016>
- [12] Maitre, J., Bouchard, K. and Bédard, L.P. (2019) Mineral Grains Recognition Using Computer Vision and Machine Learning. *Computers & Geosciences*, **130**, 84-93. <https://doi.org/10.1016/j.cageo.2019.05.009>
- [13] Singh, N., Singh, T.N., Tiway, A. and Sarkar, K.M. (2010) Textural Identification of Basaltic Rock Mass Using Image Processing and Neural Network. *Computer and Geosciences*, **14**, 301-310. <https://doi.org/10.1007/s10596-009-9154-x>
- [14] Galdames, F.J., Perez, C.A., Estévez, P.A. and Adams, M. (2017) Rock Lithological Classification by Laser Range 3D and Color Images. *International Journal of Mineral Processing*, **160**, 47-57. <https://doi.org/10.1016/j.minpro.2017.01.008>
- [15] Fan, G.P., Chen, F.X., Chen, D.Y., Li, Y. and Dong, Y.Q. (2020) A Deep Learning Model for Quick and Accurate Rock Recognition with Smartphones. *Mobile Information Systems*, **2020**, Article ID: 7462524. <https://doi.org/10.1155/2020/7462524>

- [16] Lepistö, L., Kunttu, L. and Visa, A. (2005) Rock Image Classification Using Color Features in Gabor Space. *Journal of Electronic Image*, **14**, Article ID: 040503. <https://doi.org/10.1117/1.2149872>
- [17] Vangah, J.W., Ouattara, S., Ouattara, G. and Clement, A. (2019) Global and Local Characterization of Rock Classification by Gabor and DCT Filters with a Color Texture Descriptor. *International Journal of Advanced Computer Science and Applications*, **10**. <https://doi.org/10.14569/IJACSA.2019.0100401>
- [18] Vivek, C. and Audithan, S. (2014) Robust Analysis of the Rock Texture Image Based on the Boosting Classifier with Gabor Wavelet Features. *Journal of Theoretical and Applied Information Technology*, **69**, 562-570.
- [19] Mlynarczuk, M. and Skiba, M. (2017) The Application of Artificial Intelligence for the Identification of the Maceral Groups and Mineral Components of Coal. *Computers and Geosciences*, **103**, 133-141. <https://doi.org/10.1016/j.cageo.2017.03.011>
- [20] Baklanova, O. and Shvets, O. (2014) Methods and Algorithms of Cluster Analysis in the Mining Industry—Solution of Tasks for Mineral Rocks Recognition. *Proceedings of the 11th International Conference on Signal Processing and Multimedia Applications (SIGMAP-2014)*, Vienna, 28-30 August, 2014, 165-171. <https://doi.org/10.5220/0005022901650171>
- [21] Ishikawa, S.T. and Gulick, V.C. (2013) An Automated Mineral Classifier Using Raman Spectra. *Computers & Geosciences*, **54**, 259-268. <https://doi.org/10.1016/j.cageo.2013.01.011>
- [22] Blake, D. (2012) The Development of the CheMin XRD/XRF: Reflections on Building a Spacecraft Instrument. 2012 *IEEE Aerospace Conference Proceedings*, Big Sky, 3-10 March 2012, 1-8. <https://doi.org/10.1109/AERO.2012.6187059>
- [23] Alferez, G.H., Vazquez, E.L., Martínez Ardila, A.M. and Clausen, B.L. (2021) Automatic Classification of Plutonic Rocks with Deep Learning. *Applied Computing and Geosciences*, **10**, Article ID: 100061. <https://doi.org/10.1016/j.acags.2021.100061>
- [24] Han, Q.D., Zhang, X.T. and Shen, W. (2019) Application of Support Vector Machine Based on Decision Tree Feature Extraction in Lithology Classification. *Journal of Jilin University*, **49**, 611-620.
- [25] Guo, C. and Li, Z. (2022) Automatic Rock Classification Algorithm Based on Ensemble Residual Network and Merged Region Extraction. *Advances in Multimedia*, **2022**, Article ID: 3982892. <https://doi.org/10.1155/2022/3982892>
- [26] Badeka, E., Papadopoulou, C.I. and Papakostas, G.A. (2020) Evaluation of LBP Variants in Retinal Blood Vessels Segmentation Using Machine Learning. 2020 *International Conference on Intelligent Systems and Computer Vision (ISCV)*, Fez, 9-11 June 2020, 1-7. <https://doi.org/10.1109/ISCV49265.2020.9204176>
- [27] Lepistö, L., Kunttu, L. and Visa, A. (2006) Rock Image Classification Based on k-Nearest Neighbor (K-NN) Voting. *IEEE Proceedings Vision, Image and Signal Processing*, **153**, 475-482. <https://doi.org/10.1049/ip-vis:20050315>
- [28] Marsousi, M., Abhari, K., Babyn, P. and Alirezaie, J. (2014) An Adaptive Approach to Learn Overcomplete Dictionaries with Efficient Numbers of Elements. *IEEE Transactions on Signal Processing*, **62**, 3272-3283. <https://doi.org/10.1109/TSP.2014.2324994>
- [29] Aharon, M., Elad, M. and Bruckstein, A. (2006) K-SVD: An Algorithm for Designing Overcomplete Dictionaries for Sparse Representation. *IEEE Transactions on Signal Processing*, **54**, 4311-4322. <https://doi.org/10.1109/TSP.2006.881199>